Critical Conditions for Hot Spot Evolution in Porous Explosives

B. A. Khasainov,* A. V. Attetkov,† A. A. Borisov,‡ B. S. Ermolaev,§ and V. S. Soloviev¶
USSR Academy of Sciences, Moscow USSR

Abstract

An analysis of hot spot formation and evolution in porous explosives is performed for a viscoplastic model of pore deformation behind an initiating shock wave. Critical conditions for initiation of reaction in hot spots are estimated for the limiting cases when the chemical reactions occur only in the solid phase and when they occur only in the gas phase. Based on the comparison of mean pore size in the explosive material with the critical one that is sufficient for initiating and sustaining the chemical reaction, an explanation is given of the experimental data on nonmonotonic dependence of the shock sensitivity of porous explosives on their microstructure. The dependence of the critical pore size on the initiating shock wave amplitude is presented.

Introduction

During the last decade, substantial progress was made in studies of shock initiation of porous energetic materials. Special attention has been paid to the effects of the structure of porous high explosives on their shock sensitivity [Taylor et al. (1976); Setchell and Taylor (1984); Von Holle (1983)]. Several physical models of "hot spot" generation (i.e., origination of reaction centers in

* Senior Researcher, Institute of Chemical Physics
† Senior Researcher, N. Bauman Moscow Technical University
‡ Head of Laboratory, Institute of Chemical Physics
§ Senior Researcher, Institute of Chemical Physics
¶ Professor, N. Bauman Moscow Technical University

a heterogeneous explosive), which precedes the spread of the reaction over the entire volume of shocked explosive, were developed. These models are based on the analysis of hydrodynamic and elastic-plastic interactions of an initiating shock wave (ISW) with: density discontinuities in the material, e.g., voids or solid microparticles [Mader (1979); Hayes (1983)], viscoplastic deformation of the pores caused by the action of an ISW on the material [Khasainov et al. (1981, 1983); Borisov et al. (1986); Attetkov (1986); Frey (1985); Kim and Sohn (1985); Maden (1987)] or friction heating in the shear bands [Frey (1981); Amosov (1982)].

Each of these mechanisms may lead to formation of hot spots in a suitable situation. However, theoretical studies of the stage of growth (or evolution) of the reaction centers are rather contradictory, as was demonstrated by Wackerle and Anderson (1983).

In the present work the formation and development of the reaction centers in porous explosives are analyzed based on the viscoplastic mechanism. Critical conditions for initiation of solid high explosives (HE) around a pore are calculated for the case where chemical reaction occurs in the solid phase. Within the framework of the gas-phase mechanism of chemical reaction initiation, extinguishment of certain reaction centers and transition to a self-sustained growth of the hot spot are described. The nonmonotonic dependence of the shock sensitivity of porous HE on the size of pores and HE grains (Setchell and Taylor 1984) is explained.

Dynamics of Pore Deformation

In the analysis of the dynamics of viscoplastic deformation of pores in solid materials, an effective spherical cell is usually considered (Carrol and Holt 1972). The initial radius of a void is assumed to be equal to the mean pore size a_o, and the outer radius of the cell b_o is defined in such a way that the cell porosity ϕ_o coincides with the HE porosity, i.e., $\phi_o = (a_o/b_o)^3 = 1-\rho/\rho_s$. Here ρ is the density of porous HE and ρ_s is the theoretical maximum density of the HE. Thus, in the model under consideration, the structure of the porous HE is characterized by a_o and ϕ_o.

Estimates made by Khasainov et al.(1981), indicate that, for Reynolds numbers $Re=a_o(\rho_s P_m/4\mu)^{\frac{1}{2}} < 1$ (P_m is characteristic ISW amplitude, and μ is the solid HE viscosity), the process of pore deformation behind the ISW front is viscosity-controlled and spherically symmetrical,

that is, the cell together with its field of radical velocities moves as a whole at the particle velocity behind the ISW front. This hypothesis is supported by data (Hasegawa and Fujiwara 1982) which shows that, during the course of collapse of gaseous bubbles behind a shock wave in glycerol, the shape of the bubbles is nearly spherical, even for Re ≃ 10. For propagation in the HE of a compression wave with an extended pressure profile (ramp wave), the assumption of sphericity of pore deformation is substantiated by Khasainov et al. (1983), Frey (1985), and Attetkov (1986). In both cases (sharp and ramp waves), the bulk solid in the cell may be considered to be incompressible because specific volume changes in a shocked porous material are mainly due to collapse of voids. It should be noted, however, that the real pore shape is close to the spherical one solely in high-density explosives (Soloviev et al. 1981). Shock Hugoniots of porous materials calculated employing the model of spherical cells (Dunin and Surkov 1979) are nevertheless consistent with the experimental data, even for HE densities characteristic of loosely packed materials.

The solid material is assumed to obey the relationships relevant to a viscoplastic medium. As the wave amplitude, in a porous material, $P_m(t)$, exceeds the pore strength, the pore deformation occurs in the totally plastic regime (elastic behavior of the solid material is ignored). The time history of the macroscopic pressure P_m is assumed to be prescribed. In the model suggested, a response of a porous cell to a given load is considered alone, and the effect of the processes occurring in the cell as a result of chemical reactions on the macroscopic flow pattern is not considered here, in contrast to the closed model proposed by Khasainov et al. (1981).

Inasmuch as the radial flow of the solid material around a pore arising on passage of a shock or ramp wave through the cell results in heating the solid and gas phases, this may lead to initiation of the chemical reaction.

Mechanism of Local Chemical Reaction Initiation

The analysis of the viscoplastic mechanism of hot spot formation performed by Khasainov et al. (1981, 1983) has shown that this mechanism is very efficient and provides for a temperature rise at the surface of not too small pores up to $T \geq 1000°K$ for $P_m \geq 0.5$ GPa. However, neither the melting of HE nor the detailed mechanism of chemical reactions is considered in these works.

Now we will formulate the main features of the mechanisms of chemical reactions that may occur during pore deformation. As the pore radius decreases, the temperature of the solid material at the pore surface may reach melting point. Melting points of solid explosives do not exceed 450°K at atmospheric conditions, a much lower temperature than that at which chemical decomposition becomes noticeable. Melting temperature increases nearly linearly with pressure by about 200°K per 1 GPa. With decreasing pore radius, a phase transition must occur at the pore surface. Since the pressures ($\geq$ 1 GPa) and temperatures ($\geq$300°K) under consideration are much higher than the critical point coordinates on the phase diagram of typical organic nitrocompounds, the solid material will not be converted on further heating first into liquid and then into gas. Instead, it will transfer to a new isotropic phase that for convenience is referred to below as a "gas," though under the conditions considered there is no difference between liquid and gas.

When the material is reactive, its heating during the course of pore deformation may initiate chemical reactions both in a layer of the solid adjacent to the pore surface and on the surface proper. For values of the kinetic parameters typical of solid HE pressures on the order of 1 GPa, and melting points of HE are below 700°K; at relatively low ISW amplitudes "gasification" of a solid at the surface of a pore being deformed will result from the phase transition starting when the pore surface temperature attains the melting point. At relatively high pressures $P_m \geq 3$ GPa and melting points of 1000°K, the major contribution to HE gasification results from homogeneous and heterogeneous solid-phase HE reactions occuring before the surface temperature reaches the melting point. The gaseous products evolved from the pore surface diffuse in both cases to the pore center, and their temperature finally turns out to be higher than that at the pore surface because of continuing gas compression (regardless of whether the pores have been preevacuated). As a result, an exothermic chemical reaction may also begin in the gas phase. The dynamics of the reaction center development (whether it will keep burning or fade out) is determined by the competing processes of mechanical pore deformation, heterogeneous and homogeneous solid-phase chemical reactions, and homogeneous chemical reaction and diffusion in the gaseous phase, and also by the processes of heat conduction in the gas and solid around the pore (Borisov et al. 1986).

Because of the complexity of the hot spot evolution process, it is expedient to analyze the solid-phase

(mechanism A) and gas-phase (mechanism B) mechanisms of reaction center formation and growth separately. Within the framework of mechanism A we ignored the heterogeneous reaction on the pore surface and assumed that pores contain no gas at the initial time moment and that depletion of the solid HE during the course of the chemical reaction is insignificant. Thus, the problem is reduced to determining conditions of a thermal explosion of the material around a pore being deformed by ISW (Attetkov 1986). The critical ignition phenomena are associated in mechanism A with interactions of the processes of mechanical energy dissipation, chemical heat generation, and heat transfer in the material around the pore.

In analyzing mechanism B of chemical reaction initiation in hot spots, we ignored the contribution of solid-phase chemical reactions; i.e., we assumed that the ignition takes place in the gas phase. Unlike the current version of the solid-phase ignition model, mechanism B allows the entire sequence of the processes of reaction center origination and growth up to the onset of the self-sustaining regime of pore burnout to be followed.

Mathematical Formulation of the Problem

In the frame of reference fixed at the center of a pore cell, the conservation equations for an incompressible solid viscoplastic material read as

$$\frac{\partial}{\partial r}(r^2 v_s) = 0, \quad \rho_s = \text{const}$$

$$\rho_s\left[\frac{\partial v_s}{\partial t} + v_s\frac{\partial v_s}{\partial r}\right] = \frac{\partial \sigma_r}{\partial r} + \frac{2}{r}(\sigma_r - \sigma_\theta) \tag{1a}$$

$$\rho_s c_s\left[\frac{\partial T}{\partial t}_s + v_s\frac{\partial T}{\partial r}_s\right] = (\lambda_s/r^2)\left(\frac{\partial}{\partial r} r^2\frac{\partial T}{\partial r}_s\right)$$

$$+ (2/3)(\sigma_r - \sigma_\theta)\left(\frac{\partial v_s}{\partial r} - \frac{v_s}{r}\right) + \rho_s Q_s z_s \exp(-E_s/RT_s) \tag{1b}$$

$$\sigma_r - \sigma_\theta = Y + 2\mu\,(\partial v_s/\partial r - v_s/r), \quad P_s = -(\sigma_r + 2\sigma_\theta)/3 \tag{1c}$$

$$\text{for } a(t) \le r \le b(t)$$

Here c_s, λ_s, and Y, are, respectively, the specific heat capacity, thermal conductivity, and yield strength, of solid HE, $P_s = P_s(r,t)$ is the solid-phase pressure, Q_s, z_s, and E_s are the heat, preexponential factor, and activation

energy of the chemical reaction in the solid, respectively. The thermal and physical parameters of HE are assumed to be temperature-independent, since the solid-phase temperature T_s cannot exceed melting point T_m. When the gas-phase initiation mechanism is considered, the intensity of the chemical source in the solid is set at zero.

The conservation equations for the gas phase are written as

$$\frac{\partial \rho_g}{\partial t} + \frac{1}{r^2}\frac{\partial}{\partial r}(\rho_g v_g r^2) = 0 \tag{2a}$$

$$\rho_g\left(\frac{\partial v_g}{\partial t} + v_g \frac{\partial v_g}{\partial r}\right) = -\frac{\partial P_g}{\partial r} \tag{2b}$$

$$\frac{\partial \rho_g e_g}{\partial t} + \frac{1}{r^2}\frac{\partial}{\partial r}[v_g r^2(\rho_g e_g + P_g)]$$

$$= \frac{1}{r^2}\frac{\partial}{\partial r}\left(\lambda_g r^2 \cdot \frac{\partial T_g}{\partial r}\right) + Q_g z_g \rho_g^n A^n \exp(-E_g/RT_g) \tag{2c}$$

$$\frac{\partial \rho_g A}{\partial t} + \frac{1}{r^2}\frac{\partial}{\partial r}(\rho_g v_g r^2 A) = \frac{1}{r^2}\frac{\partial}{\partial r}\left(\rho_g D\, r^2 \frac{\partial A}{\partial r}\right)$$

$$- z_g \rho_g^n A^n \exp(-E_g/RT_g) \tag{2d}$$

for $0 \le r \le a(t)$. Here A is the concentration of the gasification products evolved into pores during melting or decomposition of solid HE, D is the gas ("vapor") diffusivity, Q_g, z_g, E_g, and n are the kinetic parameters of the gas-phase reaction. The Abel equation with a constant covolume b_g was used as an equation of state of the gas phase

$$P_g(1 - b_g\rho_g) = \rho_g R_g T_g, \quad e_g = R_g T_g/(k - 1) \tag{3}$$

$$k = (c_p/c_v)_g = \text{const}$$

It should be emphasized that these equations are employed in mechanism B alone.

The conservation equations for two phases are connected by the boundary conditions at the pore surface $r = a(t)$

$$P_{s+} = P_{g+} + 2Y/3 - 4\mu v_{s+}/a + j(v_{s+} - v_{g+})$$

$$j = \rho_s(\dot{a} - v_{s+}) = \rho_g(\dot{a} - v_{g+}), \quad (\dot{a} = da/dt)$$

$$T_{s+} = T_{g+}, \quad \lambda_g(\partial T_g/\partial r)_+ = \lambda_s(\partial T_s/\partial r)_+ - jQ_m \tag{4}$$

$$D\rho_g(\partial A/\partial r)_+ = j(1 - A_+)$$

Where j is the mass rate of gasification due to solid-phase chemical reactions or phase transition at $T_{s+} = T_m$, $j = 0$ before the reaction starts or for $T_{s+} < T_m$, and $T_m = T_{mo} + C_m P$ and Q_m are the melting temperature and heat.

Boundary conditions at the pore center ($r = 0$) and at the periphery of the spherical cell [$r = b(t)$ with $b(0) = a_o/\phi_o^{1/3}$] are

$$\text{for } r = 0, \quad v_g = 0, \quad \partial T_g/\partial r = \partial P_g/\partial r = \partial A/\partial r = 0$$

$$\text{for } r = b(t), \quad \partial T_s/\partial r = 0 \tag{5}$$

The initial conditions for Eqs. (1-5) are

$$\text{for } t = 0, \quad v_s = v_g = 0, \quad P_g = P_{go},$$

$$T_s = T_g = T_o, \quad j = 0, \quad a = a_o, \quad \phi = \phi_o$$

$$\bar{P}_s(t=0) = 3\left[\int_{a_o}^{b_o} P_s r^2 dr/(b^3 - a^3)\right]_{t=0} \tag{6}$$

$$= [P_m(0) - P_{go}\phi_o]/(1 - \phi_o)$$

Equations (1) - (4) are analogous to those that describe the behavior of a gas bubble in a liquid (Nigmatulin 1978). In the present model, the response of the solid HE to compression and chemical reactions in the solid or gas phase are incorporated, and the phase transition kinetics are neglected. In particular, the temperature jump at the interface is ignored.

The pressure distribution in the solid material surrounding the pore is found by integration of the equations of solid-phase motion with respect to the radius from $a(t)$ to r, with the boundary conditions [Eq. (4)] taken into account. The mean pressure in the material around the pore $\bar{P}_s$ is found by averaging this pressure distribution over the solid phase volume. Since the mean pressure in a porous medium, also the ISW amplitude, P_m in the model considered is related to the mean pressure in the pore $\bar{P}_g$ and that in the solid material of the cell $\bar{P}_s$ by the expression

$$P_m = \bar{P}_s(1 - \phi) + \bar{P}_g\phi$$

we can establish the following equation for the motion of pore walls [from Eq. 4 it can be deduced that $v_{s+}=\dot{a} - j/\rho_s$]

$$P_m - \bar{P}_g = (2Y/3)ln(1/\phi) - (1-\phi)[4\mu v_{s+}/a - j(v_{s+} - v_{g+})]$$

$$- \rho_s\{(a\dot{v}_{s+} + 2jv_{s+}/\rho_s)[1 - \phi - 1.5(\phi^{1/3}-\phi)]$$

$$+ 1.5\, v^2_{s+}[1 - \phi - (\phi^{1/3}(2+\phi) - 3\phi)]\} \qquad (7)$$

where $\dot{v}_{s+}=dv_{s+}/dt$.

In the case of mechanism A, $\bar{P}_g=0$ and $\lambda_g=0$; hence, there is no need to use Eq. (2). For the sake of simplicity we also disregarded the effects associated with phase transitions and burning of HE before the ignition ($j = 0$ and $\dot{v}_{s+}=\dot{a}$ in this case) and assumed Y and μ to be constant. Thus, within the framework of mechanism A, the problem reduces to a solution of the heat conduction equation for the solid-phase jointly with Eq. (7). As this simplified model does not account for the generation of gaseous reaction products in the bulk of the solid material surrounding the pore, it is limited to the calculation of solely the critical ignition conditions in the vicinity of a pore being deformed. The dynamics of hot spot growth are beyond its scope.

In ignition mechanism B, the pressure in the pore is assumed to depend only on time, since the time of the pressure-wave journey in it (a_o/c_{sound}) is much less than the characteristic time of viscosity-controlled deformation of pores ($4\mu/P_m$). This assumption is equivalent to ignoring the gas motion in the pore; therefore, viscous heating was ignored in Eq. (2). Furthermore, in this model the temperature dependence of the viscosity and yield strength can also be disregarded, since the solid material temperature is bounded from above by the melting point, and Y and μ start decreasing with temperature rise only when T_s approaches T_m (Borisov et al. 1986). The heat of melting was assumed to be pressure-independent in calculations (Q_m is substantially less than heat of reaction), and the kinetic parameters for the gas-phase chemical reactions were taken equal to Q_s, z_s, and E_s, respectively (n=1).

The governing equations were solved numerically for mechanism A and approximately by the method of integral relationships for mechanism B. A comparison of the approximate calculations of pore deformation and solid heating with numerical calculations showed reasonable agreement.

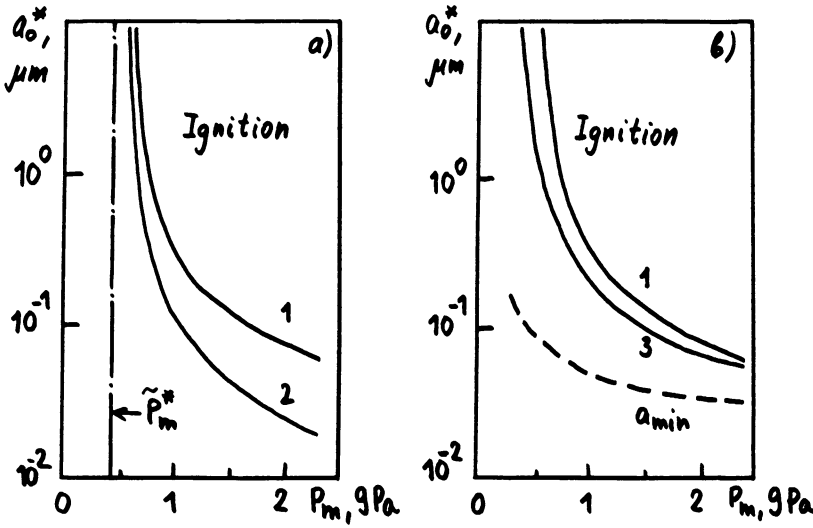

Fig. 1 The effect of viscosity (a) and yield strength (b) on the threshold of reaction initiation in TNT of initial porosity ϕ_o = 0.1. Yield strength Y = 0.2 GPa for curves 1 and 2 and 0.1 GPa for curve 3. Viscosity μ = 10 Pa-s for curves 1 and 3 and 1 Pa-s for curve 2. The dashed line in b represents the threshold pore radius at which cooling of HE by heat conduction becomes important.

Results and Discussion

To illustrate the effect of the basic parameters on the critical conditions of solid HE ignition in the vicinity of pores being deformed behind the shock wave (mechanism A) and on the ignition and growth of hot spots in mechanism B, we performed calculations for a model solid HE similar in its properties to TNT: ρ_s=1.66 g/cm^3, Q_s=4.31 MJ/m^3, E_s=0.224 MJ/mole, z_s=10^{19} s^{-1}, λ_s=0.2 W/(m°K), and C_s=1205 J/(kg°K). The viscosity of the solid HE was varied over a wide range to demonstrate the limits within which the viscoplastic model can result in reaction center growth.

Critical Conditions of Hot Spot Initiation by Mechanism A

Fig. 1 shows the critical pore size a^*_o, at which the chemical reaction can still be initiated on the pore surface as a function of the ISW amplitude for various values of the viscosity and yield strength. It is assumed that $P_m(t) = P_{mo} = const$. The explosive is ignited at a given P_m when $a_o > a^*_o$. As seen from the results presented,

the plastic properties of the solid HE dominate when the ISW amplitude is commensurate with the material strength ($P_m \simeq Y$), but for relatively strong waves ($P_m > Y$) the effect of viscosity prevails. For TNT the material strength becomes unimportant when $P_m \geq 1.5$ GPa.

The influence of structural parameters of a porous HE (a_o and ϕ_o) on the reaction initiation limit P_m^* is illustrated by the curves plotted in Fig. 2. The results show the following.

1) The structural parameters affect the initiation limit only for $P_m < 2$ GPa; at $P_m \geq 2$ GPa, practically all the pores ignite. Approximately the same pressure range ($P_m = 2.0$-2.2 GPa) was defined by Balinets and Karpukhin (1981) as the range in which the concentration of effective reaction centers reached its maximum value in TNT of the initial density $\rho = 1.66$ g/cm^3 ($\phi_o \simeq 0.06$). Taylor and Ervin (1976) considered the ISW amplitude $P_m \simeq 1.7$ GPa to be the limit of detonation initiation in TNT with $\rho = 1.56$ g/cm^3. Recent experimental studies by Balinets and Gogulya (1986) employing light-emission measurements yielded nearly the same values of the detonation initiation limit, with Pm = 2.0 GPa for pressed TNT with $\rho = 1.6$ g/cm^3 ($\phi_0 \simeq 0.036$).

2) Near the threshold wave amplitudes the effect of pore size inhomogeneity on the critical conditions for initiation of a chemical reaction in hot spots in TNT is most prominent at low porosities ($\phi_o < 0.1$). As the initial porosity of HE increases, the dependence of P_m^* on the mean pore size becomes weaker.

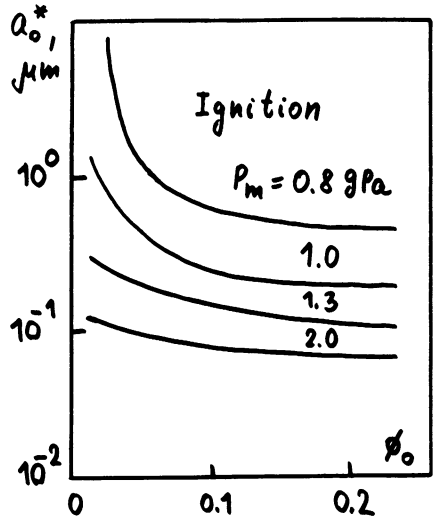

Fig. 2 Influence of structural parameters on initiation threshold of the solid-phase chemical reaction in TNT.

3) The calculated dependence of a^*_o on ISW amplitude shows that a^*_o grows abruptly with decreasing shock-wave amplitude; i.e., a threshold pressure for reaction initiation exists. Earlier we derived the following expressions for estimating this pressure:

$$P^*_m = (2Y/3)ln(1/\phi_o) + \rho_s c_s(T_{ign} - T_o)/3$$

(Khasainov et al. 1983) and

$$P^*_m = (2Y/3)ln\{1 + [(1-\phi_o)/\phi_o] \cdot \exp[(1.5\rho_s c_s(T_{ign} - T_o)/Y)^{\frac{1}{2}}]\}$$

(Attetkov 1986). Here $T_{ign} \simeq 1000°K$ is a typical temperature of pore surface ignition. The values of P^*_m in Fig. 1a are shown by the vertical bar. These two estimates agree with each other and with numerical calculations performed for mechanism A.

4) Since a decrease in the shock amplitude causes a^*_o to increase, the chemical reaction in a very porous HE (with a broad distribution of pore sizes) will be initiated by a relatively weak wave solely around sufficiently large pores. The number of such pores is greater in coarse HE. Therefore, at low shock amplitudes HE's with fine grains are less sensitive than the coarse ones having the same porosity. On the other hand, when an initiating wave is sufficiently strong (to the extent that a^*_o turns out to be much less than the mean pore size), a fine-grained HE will be more sensitive than the coarse one with the same porosity. Hence, the nonmonotonic behavior of the shock sensitivity of porous explosives as a function of their microstructure (Setchell and Taylor 1984) appears to be a natural consequence of the dependence of a^*_o on the ISW amplitude. This effect can also be accounted for based on an estimate of the threshold pore radius a_{min} at which conductive cooling of the hot spot during pore deformation becomes essential. According to Khasainov et al. (1981)

$$a_{min} = 2[m\lambda_s/(\rho_s c_s P_m)]^{\frac{1}{2}}$$

The dashed curve in Fig. 1b shows the a_{min} vs shock amplitude dependence for μ = 10 Pa-s. The a^*_o and a_{min} dependences on the shock amplitude are seen to be qualitatively similar, and their quantitative discrepancy diminishes as the shock amplitude rises and the strength of HE becomes unimportant.

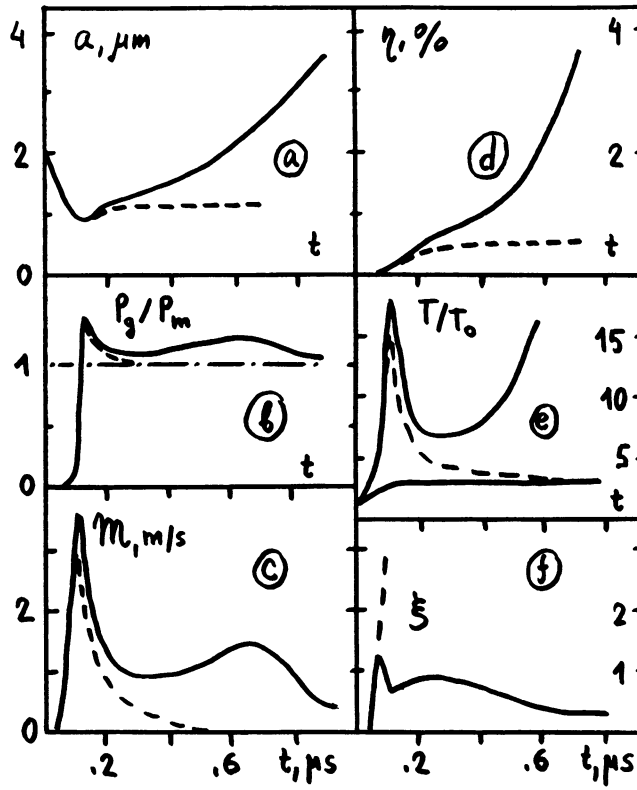

Fig. 3 Dynamics of formation and evolution of a reaction center in TNT. Results are shown for P_m=1.75 GPa, μ = 50 Pa-s, Y = 0, ϕ_o = 0.05, a_o = 2μm, k = 2, b_g = 1 cm^3/g, W_g = 22.7 g/mole, D = $\lambda_g/\rho_g c_g$, λ_g = 0.08 W/(m·K), the constants in dependence of melting point on pressure $T_m = T_{mo} + C_m P$: T_{mo} = 478°K, C_m = 200°K/GPa, and Q_m = 1 MJ/Kg, with (solid curve) and without (dashed lines) gasphase decomposition of TNT.

Development of Reaction Centers According to Mechanism B

In Fig. 3 the evolution of a reaction center is shown with and without allowance for the gas-phase exothermic reaction of TNT "vapor" in a hot spot formed in an HE charge loaded with a long-duration shock wave. The results diverge only after vapor ignition occurs. First, we discuss the case of inert vapors. At the initial stage of pore deformation a reduction of its radius (Fig. 3a) is accompanied by a rise of the pore surface temperature (the bottom curve in Fig. 3e) and the gas temperature [the medium-dashed curve in Fig. 3e represents a temperature of gas in the center of the pore, $T_g(r=0)$]. At t=0.07μs the

pore surface temperature reaches the melting point and the phase transition starts, as a result of which vapors of the solid material begin to flow into the pore and thus enhance the pressure rise in the pore (Fig. 3b). The linear regression rate for the solid undergoing the phase transition is shown in Fig. 3c by the dashed curve. The dimensionless parameter ξ, inversely proportional to the gradient of vapor concentration at the pore surface, is presented in Fig. 3f. In the absence of the chemical reaction in the gas, the vapors rapidly fill the pore volume, and their concentration becomes almost uniformly distributed (dashed curve). Characteristics of this stage are a fast rise of the gas pressure, regression rate, and gas temperature in the pore center. The mass fraction of gasified solid material η also grows (Fig. 3d). The pore pressure becomes even higher than the mean pressure P_m in the two-phase medium; therefore, the pore radius ceases to grow and the pore starts to expand (Fig. 3a) at the expense of both the phase transition and the pressure difference. This immediately causes a pressure decay in the pore to the ambient pressure, which in turn leads to a drop of the temperature in the pore and of the regression rate (Figs. 3e and 3c) and η to level off (fig. 3d). Finally the gas temperature drops to the melting point as the result of pore expansion and injection into the pore of a large amount of relatively cold gas at $T_{g+} = T_m$, and solid gasification stops. Starting with this instant (about 0.6μs), the surface layers of the pore are slowly cooled by heat conduction in the solid phase. Because of the phase transition of an inert material, about 0.5% of it converts into gas during pore deformation.

The situation is quite different for reactive vapors. Almost immediately after gasification begins, HE vapors diffuse to the pore center, where the high temperature ignites them. As a result, the vapor front appears as if it is pushed backward to the pore surface (Fig. 3f, solid line) because of the burning of the vapor. With exothermic reaction in the pore the pore pressure and temperature do not drop as rapidly as in the case of inert vapor. The gas temperature then grows to a high value and causes the regression rate to increase (Fig. 3c). After a relaxation period, from 0.1 to 0.8 μs, the regression rate attains a quasisteady value of about 0.4 m/s, and the reaction center grows further in a self-sustaining regime.

The burnt fraction of the HE as a function of time during pore deformation is shown in Fig. 4 for various shock-wave amplitudes. Although the characteristic reaction center burnout times may differ appreciably,

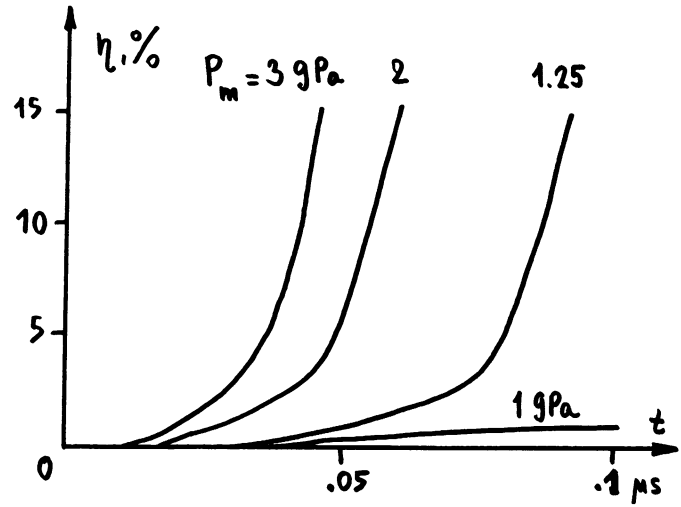

Fig. 4 Burnt fractions of TNT vs time for different shock-wave amplitudes. Results are for: μ = 10 Pa-s, a_o = 1 μm, and k = 2.

depending on values of the main parameters, the time histories of the burnt fractions possess some common features. A critical shock amplitude exists below which no self-sustaining chemical reaction is initiated in the hot spot. In the examples considered this critical pressure is close to 1 GPa, in reasonable agreement with the experimental data [Taylor and Ervin (1976); Balinets and Karpukhin (1981); Balinets and Gogulya (1986)]. The results (Fig. 4) suggest that decomposition of HE around the pore occurs in two stages corresponding to the clearly distinguished portions of the η (t) curves with fundamentally different sensitivities to the shock amplitude. In the initial stage (up to burnt fractions of the order of a few percentage points) the hot-spot burnout dynamics is strongly dependent on the shock amplitude. After the quasisteady self-sustaining regime is attained, the burning rate is only slightly affected by the shock strength. This result agrees qualitatively with the experimental data (Von Holle and Tarver 1981) and can be explained by the fact that, at the pressures considered, the gas density grows only slightly with the growth of pressure, and the burning velocity increases with the rising gas density. At the reaction initiation limit the burnt fraction of the solid HE ($\eta \approx 1\%$) may be sufficient to sustain propagation regimes of low velocity detonations (Khasainov et al. 1977). Calculations also show an

interesting effect; namely, in some cases an increase of P_m enhanced HE burning up to $\eta \simeq 15$-30% only. After this the burning rate vs P_m dependence for a growing hot spot is reversed. This result may indicate that the solid-phase reaction should be incorporated into the model.

Figure 5 demonstrates η (t) dependence for various initial pore radii a_0. The smaller the mean pore size, i.e., the higher the HE-specific surface for a fixed value of porosity ($\phi_0 = 0.05$ in the case of issue), the faster the reaction center grows. This trend is observed only for mean pore sizes exceeding the critical value $a^*_o \approx a_{min}$. For example, at $a_o = 0.3\mu m$ the chemical reaction cannot be initiated with the other parameters being equal. Thus, the gas-phase ignition mechanism also may explain the nonmonotonic dependence of shock sensitivity of porous explosives on their microstructure.

The time histories of the burnt fraction and gas pressure in the pore, for the case when the porous HE is pressurized by a shock wave and ramp compression wave with an extended front of the same amplitude (2.5 GPa), are

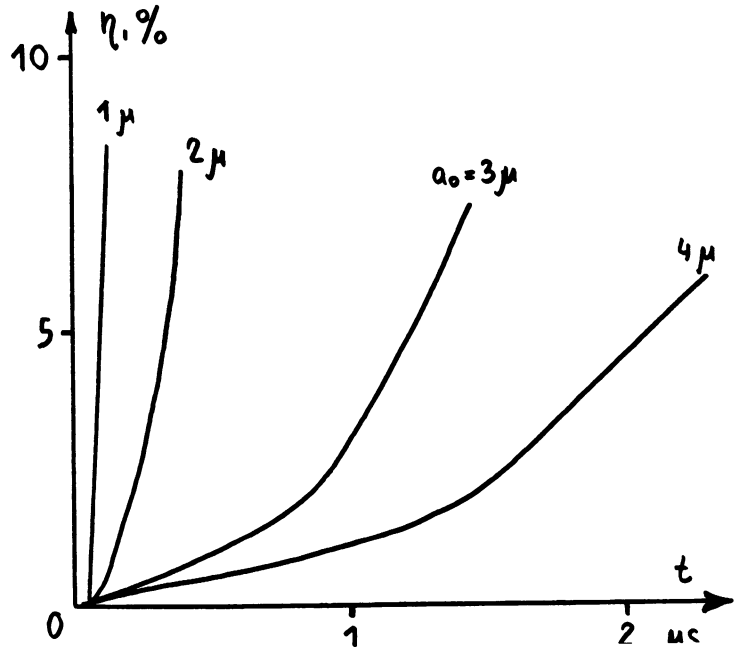

Fig. 5 Burnt fractions of TNT vs time for shock wave initiation at different values of the mean pore size. Results are for $P_m = 2.5$ GPa and $\mu = 100$ Pa-s

presented in Fig. 6. The calculations demonstrate that viscosity increases result in longer hot spot ignition delays, since a_{min} rises as the viscosity grows and may become commensurate with a_o. The pressure in the pore after ignition also increases, since the forces resisting the pore expansion increase. In a wave with a longer rise time (2 μs instead of 1 μs), the reaction centers form much

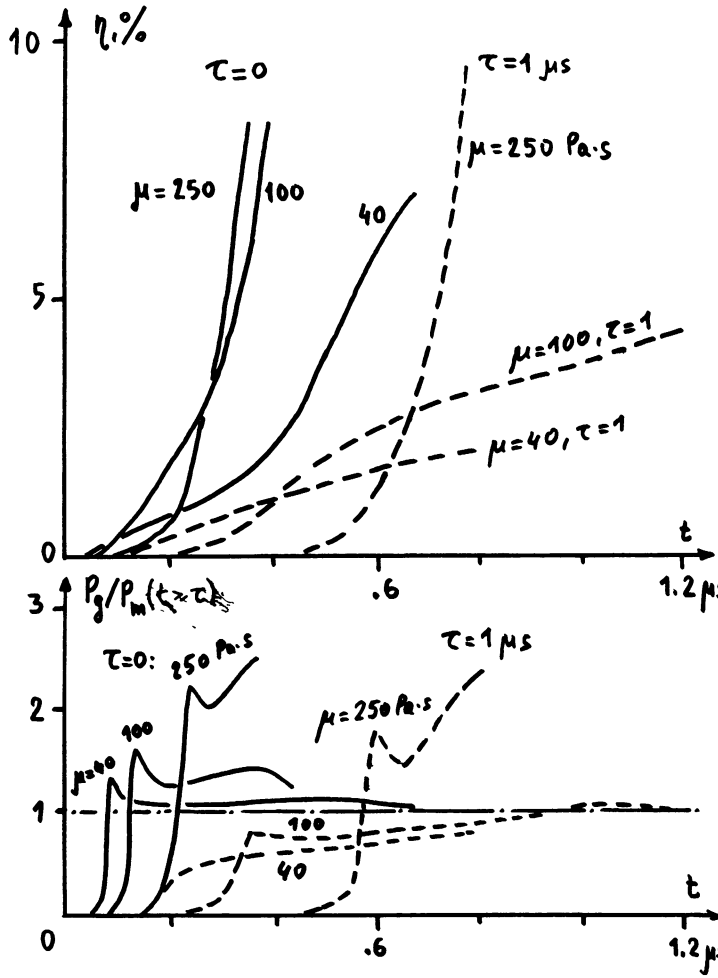

Fig. 6 Comparison of burnt fractions vs time curves for porous TNT (ϕ_o = 0.05) of various viscosity loaded by a shock and compression waves of the same amplitude (2.5 GPa). The pressure in the ramp wave changes stepwise to 0.5 GPa at time zero [to provide $P_m(t=0) > (2Y/3)ln(1/\phi_o)$] and then to grow linearly with time to 2.5 GPa for τ = 1 and 2 μs.

more slowly, and, when τ = 2μs and μ = 40 Pa-s, no reaction is initiated in the hot spot.

Additional calculations with gas heat conductivity set at zero show that at the initial stage of pore deformation thermal conduction from the gas phase contributes little to solid phase heating. During this time the gas pressure is much lower than the solid phase one (i.e., the HE is heated at the expense of the viscous energy dissipation and the work of plastic deformation). After the gas and solid pressure become equal, the energy is transferred to the fresh solid around the pore solely by gas-phase heat conduction rather than by viscous energy dissipation. If the HE strength is taken into account, the gas pressure at the stage of self-sustaining hot spot growth exceeds the solid-phase pressure by $(2Y/3)ln(1/\phi) \approx$ 0.1 GPa; v_{s+} in this case is nearly zero. The proposed model ignores the compressibility of solid HE and hence the possible role of hydrodynamic flow in the energy transfer mechanism. After postignition pressure relaxation in the gas phase, heat conduction becomes the major energy transfer mechanism from the gas to the solid in the model considered.

Summary

The main results of the computations are as follows:
1) The gas-phase ignition mechanism may describe both the development of a reaction center (from ignition to self-sustaining burning) and its extinction.
2) The two ignition mechanisms considered explain the experimentally observed nonmonotonic dependence of shock sensitivity of porous high explosives on grain and pore size through a comparison of the mean pore size with the critical one at which the self-sustaining chemical reaction can still be initiated in the hot spot. This critical pore size increases when the amplitudes of constant or ramped strength shock waves decline.
3) According to the gas-phase initiation mechanism, the rate of reaction center growth is determined by the initiating wave amplitude at the initial stage of the reaction but is practically independent of wave amplitude when the burnt fraction of the solid explosive around the pore exceeds several percentage points. This prediction is also consistent with the experimental data.
4) The model suggested may be employed in modeling detonation buildup (particularly low-velocity detonations) and estimating critical pressures of local chemical reaction initiation in porous high explosives behind shock and compression waves.

References

Amosov, A. P. (1982) Heating and ignition of solid reactive systems due to high velocity friction accompanied by formation of plastic and liquid layers. Khim. Fiz. 1, 1401.

Attetkov, A. V. (1986) Critical conditions of chemical reaction initiation in solid heterogeneous substances. Sixth Soviet Congress on Theoretical and Applied Mechanics. Abstracts, Tashkent, USSR, Vol. 57.

Balinets, Y. M. and Karapukhin, I. A. (1981) On initial stage of detonation initiation process in pressed TNT. Fiz. Goreniya Vzryva, 17, 103.

Balinets, Y. M. and Gogulya, M. F. (1986) Emissivity of shocked charges of pressed TNT. Khim Fiz. 5, 263.

Borisov, A. A., Ermolaev, B. S., and Khasainov, B. A. (1986) The model of hot spot growth during visco-plastic pore deformation. Sixth Soviet Congress on Theoretical and Applied Mechanics. Abstracts, Tashkent, USSR, Vol. 129.

Carrol, M. M. and Holt, A. C. (1972) Static and dynamic pore-collapse relations for ductile porous materials. J. Appl. Physiol., 43, 1626.

Dunin, S. Z. and Surkov, V. V. (1979) Structure of a shock wave front in a porous solid. Zh. Prikl. Mekh. Tekh. Fiz., 5, 106.

Frey, R. B. (1981) The initiation of explosive charges by rapid shear. Seventh Symposium (International) on Detonation, NSWC MP 82-334, p. 36.

Frey, R. B. (1985) Cavity collapse in energetic materials. Eighth Symposium (International) on Detonation, Preprints of papers, CONF-850706, Vol. 1, p. 385.

Hasegawa, T. and Fujiwara, T. (1982) Detonation in oxyhydrogen bubbled liquids. 19th Symposium (International) on Combustion, The Combustion Institute, Pittsburgh, PA, p. 675.

Hayes, D. B. (1983) Shock induced hot-spot formation and subsequent decomposition in granular, porous HNS explosive. Progress in Astronautics and Aeronautics: Shock Waves, Explosions, and Detonations, Vol. 87, edited by J. R. Bowen, N. Manson, A. K. Oppenheim, and R. I. Soloukhin, 445-467.

Khasainov, B. A., Ermolaev, B. S., Borisov, A. A., and Korotkov, A. I. (1977) Low velocity detonations in high density high explosives. Khimicheskaya Fizika Protsessov Goreniya i Vzryva Detonatsya, Chernogolovka, USSR, p. 79.

Khasainov, B. A., Borisov, A. A., Ermolaev, B. S. and Korotkov, A. I. (1981) Two-phase viscoplastic model of shock initiation of detonation in high density pressed explosives. Seventh Symposium (International) on Detonation, NSWC MP 82-334, p. 435.

Khasainov, B. A., Borisov, A. A. and Ermolaev, B. S. (1983) Shock wave predetonation processes in porous high explosives. AIAA Progress in Astronautics and Aeronautics: Shock Waves, Explosions, and Detonations, Vol. 87, edited by J. R. Bowen, N. Manson, A. K. Oppenheim, and R. I. Soloukhin, AIAA, New York, pp 492-504.

Kim K. and Sohn, C. H. (1985) Modeling of reaction build-up processes in shocked porous explosives. Eighth Symposium (International) on Detonation, Preprints of papers, CONF-850706, Vol. 2, p. 641.

Maiden, D. E. (1987) A model for calculating the threshold for shock initiation of pyrotechnics and explosives, 12th International Pyrotechnic Seminar, France, p. 17.

Mader, C. L. (1979) Numerical Modeling of Detonations. Univ. of California Press, Berkeley, CA.

Nigmatullin, R. I. (1978) Fundamentals of Heterogeneous Media Mechanics, Nauka, Moscow.

Setchell, R. E. and Taylor, P. A. (1984) The effects of grain size on shock initiation mechanisms in Hexanitrostilbene (HMX) explosive. Progress in Astronautics and Aeronautics: Shock Waves, Explosives, and Detonations, Vol. 94, edited by J. R. Bowen, N. Manson, A. K. Oppenheim, and R. I. Soloukhin, AIAA, New York, 350-368.

Soloviev, V. S., Attetkov, A. V., and Pyriev, V. A. (1981) Investigation of cast explosive microstructure. Detonatsya. Materialy Vses. Soveshchanya po Deonatsii. Chernogolovka, USSR, Vol. 2, p. 61.

Taylor, B. C. and Ervin, L. H. (1976) Separation of ignition and buildup to detonation in pressed TNT. Sixth Symposium (International) on Detonation, Office of Naval Research, ACR-221, p. 3.

Von Holle, W. G. and Tarver, C. M. (1981) Temperature measurements of shocked explosives by time-resolved infrared radiometry - a new technique to measure shock induced reaction. Seventh Symposium (International) on Detonation, NSWC MP 82-334, p. 993.

Von Holle, W. G. (1983) Shock wave diagnostics by time resolved infrared radiometry and nonlinear Raman spectroscopy. Shock Waves in Condensed Matter. Proceedings of the American Physical Society Topical Conference, p. 283.

Wackerle, J. and Anderson, A. B. (1983) Burning topology in the shock induced reaction of heterogeneous explosives. Shock Waves in Condensed Matter. Proceedings of the American Physical Society Topical Conference, p. 601.